Stability conditions and phase diagrams for two component Fermi gases with population imbalance

Qijin Chen, Yan He, Chih-Chun Chien, and K. Levin

James Franck Institute and Department of Physics, University of Chicago, Chicago, Illinois 60637, USA
(Dated: February 6, 2008)

Superfluidity in atomic Fermi gases with population imbalance has recently become an exciting research focus. There is considerable disagreement in the literature about the appropriate stability conditions for states in the phase diagram throughout the BCS to Bose-Einstein condensation (BEC) crossover. Here we discuss these stability conditions for homogeneous polarized superfluid phases, and compare with recent alternative proposals. The requirement of a positive second order partial derivative of the thermodynamic potential with respect to the fermionic excitation gap Δ (at fixed chemical potentials) is demonstrated to be equivalent to the positive definiteness of the particle number susceptibility matrix. In addition, we show the positivity of the effective pair mass constitutes another nontrivial stability condition. These conditions determine the stability of the system towards phase separation of one form or another. We also study systematically the effects of finite temperature and the related pseudogap on the phase diagrams defined by our stability conditions.

PACS numbers: 03.75.Hh, 03.75.Ss, 74.20.-z **cond-mat/0608454**

I. INTRODUCTION

Superfluidity in atomic Fermi gases has become an important research arena [1, 2, 3, 4, 5, 6, 7, 8] for both the condensed matter and atomic, molecular and optical physics communities. In these ultracold gases, via a Feshbach resonance, one can tune the pairing interaction strength continuously from very weak in the BCS limit to very strong in the Bose-Einstein condensation (BEC) limit. Adding greatly to the excitement has been a recent emphasis on experimental studies of superfluidity [9, 10, 11] in the presence of a population imbalance between the two fermion spin components. This system has important consequences for other subfields of physics including nuclear physics and high density QCD [12, 13, 14]. From a theoretical standpoint this problem is particularly rich and at the same time complex [15, 16, 17, 18, 19, 20, 21, 22, 23]. Simple mean-field calculations [24] show that, unlike in the equal spin mixture case, a homogeneous superfluid state is not always a stable ground state at zero temperature (T). There are a number of different ground states to consider. Moreover, there has been considerable controversy in the literature [21, 24, 25, 26] about the precise nature of the stability conditions, associated with one mean-field ground state or another.

It, thus, becomes particularly important to characterize and study the stability conditions associated with polarized superfluids. Moreover, since there is a natural extension [24, 27, 28, 29, 30] of the standard ground states to finite temperatures T, in this paper, we derive these stability conditions for a homogeneous interacting Fermi gas superfluid with population imbalance throughout the entire BCS-BEC crossover, and at arbitrary T. We will focus our attention on a superfluid composed of a condensate of pairs which has a zero total center-of-mass momentum. Therefore, we will not discuss the Fulde-Ferrell-Larkin-Ovchinnikov (FFLO) state [31], which allows condensation of pairs at finite momenta. It appears that the FFLO state with pairing at only one value of momentum $\mathbf{q}_0$ is stable only in a very limited phase space [32]. Multiple plane wave FFLO states are much more complicated and are currently under investigation.

We set up the central issues of this paper by summarizing our previously obtained [24] results on the zero temperature phase diagram in the p–$1/k_Fa$ plane plotted in Fig. 1. Here $p \equiv \delta N/N$ is the polarization, k_F is the Fermi wavevector of a noninteracting Fermi gas of the same number density without a population imbalance, a is the two-body s-wave scattering length, $N = N_\uparrow + N_\downarrow$ and $\delta N = N_\uparrow - N_\downarrow > 0$ are the total number and number difference, respectively. In the BCS limit, our result for the boundary separating the stable polarized normal Fermi gas and the unstable Sarma phase agrees with that in Ref. [25], but differs quantitatively from that in Ref. [26]. On the BEC side, our result agrees with that of Ref. [26] but not that of Ref. [25]. Since there is so much controversy in the literature, this paper, then, addresses a particularly timely issue.

The differences between the various theoretical proposals for the phase diagram stem from different conclusions concerning the stability of the various phases. There seems to be general agreement [21, 24, 26] about the two generic stability requirements which were first articulated in Ref. [25] where it was argued that the number susceptibility matrix must have positive eigenvalues, and that the superfluid density must also be positive. We will show in detail here that in contrast to Ref. [26], that the positivity of eigenvalues of the number susceptibility matrix is equivalent to the positivity of the 2nd order partial derivative $\frac{\partial^2\Omega}{\partial\Delta^2}$, where Ω is the thermodynamic potential, and Δ the fermionic excitation gap. The same observation was very recently made in Ref. [21]. In comparison to these two equivalent conditions, we find that the positivity requirement on the superfluid density is much less stringent. This differs from Ref. [21] but agrees with Refs. [25, 26]. In addition, we find that the requirement that the pair mass be positive constitutes another nontrivial stability condition, and may be more stringent than the positivity of $\frac{\partial^2\Omega}{\partial\Delta^2}$ at low temperature and low imbalance in the BCS regime.

Our theoretical formalism is described in Ref. [24], so we will not repeat the details here. The system is composed of two spin components of number $N_\uparrow$ and $N_\downarrow$ and of chemical potential $\mu_\uparrow$ and $\mu_\downarrow$, respectively. They interact via the attrac-

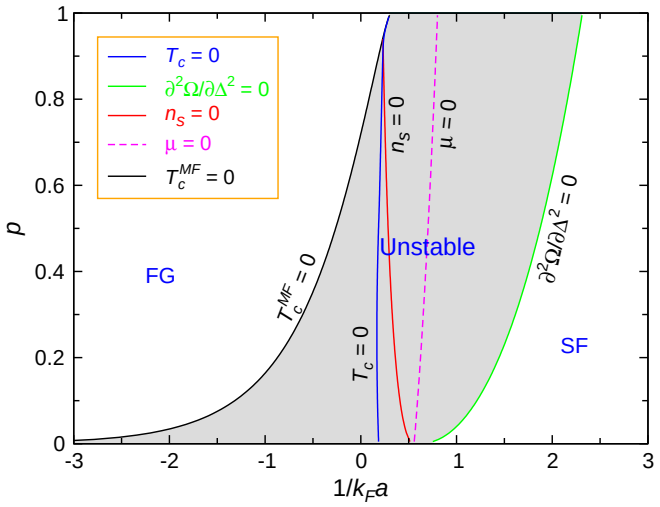

FIG. 1: Zero temperature phase diagram of a homogeneous Fermi gas as a function of pairing interaction characterized by $1/k_Fa$ and the polarization p. On the left side of the (black) $T_c^{MF} = 0$ curve, the system is a stable polarized Fermi gas (labeled by "FG"). On the right side of the (green) $\partial^2\Omega/\partial\Delta^2 = 0$ curve, the system is a stable polarized superfluid at low T, labeled by "SF". At $T = 0$, the entire shaded region between these two curves is unstable against phase separation, and a stable polarized superfluid can exist only in the BEC regime. The (red) $n_s = 0$ curve and the (blue) $T_c = 0 = 1/M^*$ curves are completely within the unstable regime. Here k_F is the Fermi wavevector of a noninteracting two component Fermi gas of the same density n without a population imbalance. All energies are measured in units of $E_F \equiv k_F^2/2m$. Throughout this paper, we use $k_0 = 80k_F$.

tive interaction $U_{\mathbf{k},\mathbf{k}'} = U\varphi_{\mathbf{k}}\varphi'_{\mathbf{k}}$ with $U < 0$. Here we use a Gaussian cutoff $\varphi_{\mathbf{k}} = e^{-k^2/2k_0^2}$ with k_0 sufficiently large (as appropriate for a short range potential). The cutoff $\varphi_{\mathbf{k}}$ can be used to approximate a potential, which includes but also generalizes the well studied contact potential. Here k_0 is given by the inverse range of interaction, and we take $k_0 = 80k_F$ in our numeric calculations throughout this paper. This interaction is related to $1/k_Fa$ via $m/4\pi a = 1/U + \sum_{\mathbf{k}} \varphi_{\mathbf{k}}^2/2\epsilon_{\mathbf{k}}$, where $\epsilon_{\mathbf{k}} = k^2/2m$. The full fermion Green's function is given by $G_{\uparrow,\downarrow}(K) = u_{\mathbf{k}}^2/(i\omega_n \pm h - E_{\mathbf{k}}) + v_{\mathbf{k}}^2/(i\omega_n \pm h + E_{\mathbf{k}})$, where $E_{\mathbf{k}} = \sqrt{\xi_{\mathbf{k}}^2 + \Delta^2}$, $\xi_{\mathbf{k}} = \epsilon_{\mathbf{k}} - \mu$, $\mu = (\mu_\uparrow + \mu_\downarrow)/2$, $h = (\mu_\uparrow - \mu_\downarrow)/2$ and $u_{\mathbf{k}}^2, v_{\mathbf{k}}^2 = (1 \pm \xi_{\mathbf{k}}/E_{\mathbf{k}})/2$. As in Ref. [24], we set the volume $V = 1$, $\hbar = k_B = 1$, and $K \equiv (i\omega_n, \mathbf{k})$, $Q \equiv (i\Omega_m, \mathbf{q})$, $\sum_K \equiv T\sum_n \sum_{\mathbf{k}}$, etc, where $\omega_n(\Omega_m)$ is odd (even) Matsubara frequencies [33]. Our Green's function is equivalent to presuming the BCS form for the self-energy, $\Sigma_\sigma(K) = -\Delta^2 G_{\bar\sigma}^0(-K)\varphi_{\mathbf{k}}^2$, where $\sigma = \uparrow, \downarrow$ and $\bar\sigma = -\sigma$. Here the bare Green's function $G_{0,\sigma}^{-1}(K) = i\omega_n - \xi_{\mathbf{k},\sigma}$. With these definitions we introduce the important pair susceptibility

$$\chi(Q) = \sum_K G(K)G_0(Q-K)\varphi^2_{\mathbf{k}-\mathbf{q}/2}, \tag{1}$$

which enters throughout the present paper. We thus have $\sum_K \Sigma_\sigma(K)G_\sigma(K) = -\Delta^2\chi(0)$,

At finite T, we have four equations in the presence of population imbalance. They are the gap (Δ) equation, two number equations, and the pseudogap (Δ_{pg}) equation. At zero T (where $\Delta_{pg} = 0$), our theory yields three equations and reduces to the standard one-channel results in the literature. More generally $\Delta^2(T) = \Delta_{sc}^2(T) + \Delta_{pg}^2(T)$, where Δ_{sc} is the superfluid order parameter. Except for the number difference equation, all equations can be written in the same form as in the case with equal spin population [28], provided one replaces the Fermi distribution function $f(x)$ and its derivative $f'(x)$ with the averages $\bar f(x) \equiv [f(x+h) + f(x-h)]/2$ and $\bar f'(x)$. At $T \neq 0$, we must include the effects of noncondensed pairs via the pseudogap term Δ_{pg}. These noncondensed pairs have been ignored in previous work [21, 34, 35], and are found to be extremely important here. They have an effective pair mass M^* which must necessarily be positive, thereby, adding another condition to the requirements for phase stability.

At general T, our self consistent equations are

$$0 = 1 + U\chi(0) = 1 + U\sum_{\mathbf{k}} \frac{1 - 2\bar f(E_{\mathbf{k}})}{2E_{\mathbf{k}}}\varphi_{\mathbf{k}}^2\,, \tag{2}$$

$$n = 2\sum_{\mathbf{k}} \left[v_{\mathbf{k}}^2 + \frac{\xi_{\mathbf{k}}}{E_{\mathbf{k}}}\bar f(E_{\mathbf{k}}) \right], \tag{3a}$$

$$pn = \sum_{\mathbf{k}} [f(E_{\mathbf{k}} - h) - f(E_{\mathbf{k}} + h)] \tag{3b}$$

$$\Delta_{pg}^2 \equiv -\sum_{Q\neq 0} t(Q) = \frac{1}{Z}\sum_{\mathbf{q}} b(\Omega_{\mathbf{q}})\,, \tag{4}$$

Here $\chi(0)$ is the pair susceptibility at $Q = 0$, and $\Omega_{\mathbf{q}} = q^2/2M^*$ is the pair dispersion. From Eq. (3b), we have $h > \Delta$ at $T = 0$ for any $p > 0$. Solving Eqs. (2)-(3) with $\Delta = 0$ at $T = 0$, we can obtain the boundary between the polarized normal Fermi gas phase and the unstable phase in Fig. 1.

II. THERMODYNAMIC POTENTIAL Ω

We first discuss the gap [Eq. (2)] and number equations [Eqs. (3)], which govern the fermionic degrees of freedom, and only later address pseudogap effects which appear at finite T through Eq. (4). The gap and number equations can be obtained from the fermionic part of the thermodynamic potential $\Omega(\Delta, \mu, h)$ via partial derivatives with respect to Δ, μ, and h, respectively. It should be noted that only the gap equation corresponds to a vanishing first order derivative.

Instead of writing down the thermodynamic potential from the known quasiparticle energy spectra [16], we calculate it via the energy and entropy. We have

$$K \equiv E - \mu_\uparrow N_\uparrow - \mu_\downarrow N_\downarrow = E - \mu N - h\delta N, \tag{5a}$$

$$\Omega \equiv E - TS - \mu N - h\delta N = K - TS\,, \tag{5b}$$

$$F \equiv E - TS = \Omega + \mu N + h\delta N\,, \tag{5c}$$

and

$$N = -\left(\frac{\partial\Omega}{\partial\mu}\right)_{\Delta,h}, \qquad \delta N = -\left(\frac{\partial\Omega}{\partial h}\right)_{\Delta,\mu}. \quad (6)$$

The energy for each spin is given by

$$E_\sigma = \sum_K \left[\epsilon_{\mathbf{k}} + \frac{1}{2}\Sigma_\sigma(K)\right] G_\sigma(K). \quad (7)$$

Using the gap equation (2), one can show that

$$\begin{aligned} E &= \sum_\sigma E_\sigma = \sum_K \epsilon_{\mathbf{k}}[G_\uparrow(K) + G_\downarrow(K)] - \Delta^2\chi(0) \\ &= \sum_{\mathbf{k}} \left[\xi_{\mathbf{k}} - E_{\mathbf{k}} + 2E_{\mathbf{k}}\bar{f}(E_{\mathbf{k}})\right] + \mu N - \frac{\Delta^2}{U}, \quad (8) \\ K &= \sum_{\mathbf{k}} \left[\xi_{\mathbf{k}} - E_{\mathbf{k}} + 2E_{\mathbf{k}}\bar{f}(E_{\mathbf{k}})\right] - h\delta N - \frac{\Delta^2}{U}. \quad (9) \end{aligned}$$

The quasiparticle excitation energies are now given by $\pm E_{\mathbf{k}} + \sigma h$, where $\sigma = \pm 1$ for spin down and up, respectively. The entropy contains contributions from both spin species.

$$\begin{aligned} S = &- \sum_{\sigma=\pm 1}\sum_{\mathbf{k}} [f(-E_{\mathbf{k}} + \sigma h)\ln f(-E_{\mathbf{k}} + \sigma h) \\ &+ f(E_{\mathbf{k}} + \sigma h)\ln f(E_{\mathbf{k}} + \sigma h)]. \quad (10) \end{aligned}$$

$$\frac{\partial K}{\partial\Delta} = \sum_{\mathbf{k}} [2E_{\mathbf{k}}\bar{f}'(E_{\mathbf{k}}) + 2\bar{f}(E_{\mathbf{k}}) - 1]\frac{\partial E_{\mathbf{k}}}{\partial\Delta} - h\frac{\partial\delta N}{\partial\Delta} - 2\frac{\Delta}{U}$$

$$\frac{\partial S}{\partial\Delta} = \frac{2}{T}\sum_{\mathbf{k}} \bar{f}'(E_{\mathbf{k}})E_{\mathbf{k}}\frac{\partial E_{\mathbf{k}}}{\partial\Delta} - \frac{h}{T}\frac{\partial\delta N}{\partial\Delta}$$

Finally, we obtain

$$\begin{aligned} \frac{\partial\Omega}{\partial\Delta} &= \frac{\partial K}{\partial\Delta} - T\frac{\partial S}{\partial\Delta} = \sum_{\mathbf{k}} \left[2\bar{f}(E_{\mathbf{k}}) - 1\right]\frac{\partial\delta N}{\partial\Delta} - 2\frac{\Delta}{U} \\ &= -\frac{2\Delta}{U}\left[1 + U\chi(0)\right], \quad (11) \end{aligned}$$

where we have used the relationship $\partial E_{\mathbf{k}}/\partial\Delta = \Delta\varphi_{\mathbf{k}}^2/E_{\mathbf{k}}$. It is evident that when the gap equation is satisfied, $\partial\Omega/\partial\Delta = 0$. Alternatively, one easily finds $\mathrm{d}F/\mathrm{d}\Delta = 0$ at the same time. It is interesting to note that in Eq. (5c) the term μN cancels that from E, whereas $h\delta N$ cancels that in TS. It is straightforward to verify Eqs. (6) are equivalent to the usual form of the number and number difference equations (3a) and (3b). Using Eqs. (6),

When the gap equation is satisfied, we readily obtain

$$\begin{aligned} \frac{\partial^2\Omega}{\partial\Delta^2} &= -2\left[\frac{1}{U} + \chi(0)\right] - 2\Delta\frac{\partial\chi(0)}{\partial\Delta} \\ &= 2\sum_{\mathbf{k}} \frac{\Delta^2\varphi_{\mathbf{k}}^4}{E_{\mathbf{k}}^2}\left[\frac{1 - 2\bar{f}(E_{\mathbf{k}})}{2E_{\mathbf{k}}} + \bar{f}'(E_{\mathbf{k}})\right]. \quad (12a) \end{aligned}$$

Additional second order partial derivatives of interest are

$$\begin{aligned} \frac{\partial^2\Omega}{\partial\mu\partial\Delta} &= -2\sum_{\mathbf{k}} \frac{\Delta\epsilon_{\mathbf{k}}\varphi_{\mathbf{k}}^2}{E_{\mathbf{k}}^2}\left[\frac{1 - 2\bar{f}(E_{\mathbf{k}})}{2E_{\mathbf{k}}} + \bar{f}'(E_{\mathbf{k}})\right] \\ &= -\frac{\partial N}{\partial\Delta}, \quad (12b) \\ \frac{\partial^2\Omega}{\partial\mu\partial h} &= \sum_{\mathbf{k}} \frac{\epsilon_{\mathbf{k}}}{E_{\mathbf{k}}}\left[f'(E_{\mathbf{k}} - h) - f'(E_{\mathbf{k}} + h)\right] \\ &= -\frac{\partial N}{\partial h} = -\frac{\partial\delta N}{\partial\mu}, \quad (12c) \\ \frac{\partial^2\Omega}{\partial\Delta\partial h} &= -\sum_{\mathbf{k}} \frac{\Delta\varphi_{\mathbf{k}}^2}{E_{\mathbf{k}}}\left[f'(E_{\mathbf{k}} - h) - f'(E_{\mathbf{k}} + h)\right] \\ &= -\frac{\partial\delta N}{\partial\Delta}, \quad (12d) \\ \frac{\partial^2\Omega}{\partial\mu^2} &= -\frac{\partial N}{\partial\mu} = 2\sum_{\mathbf{k}} \left\{\bar{f}'(E_{\mathbf{k}}) \right. \\ &\quad \left. - \frac{\Delta^2\varphi_{\mathbf{k}}^2}{E_{\mathbf{k}}^2}\left[\frac{1 - 2\bar{f}(E_{\mathbf{k}})}{2E_{\mathbf{k}}} + \bar{f}'(E_{\mathbf{k}})\right]\right\}, \quad (12e) \\ \frac{\partial^2\Omega}{\partial h^2} &= -\frac{\partial\delta N}{\partial h} = 2\sum_{\mathbf{k}} \bar{f}'(E_{\mathbf{k}}). \quad (12f) \end{aligned}$$

III. STABILITY CONDITIONS

A. Stability of the polarized normal phase on the BCS side

The condition $\partial\Omega/\partial\Delta = 0$ admits a trivial solution $\Delta = 0$. Referring now to Fig. 1, we see that on the *left side* of the boundary $T_c^{MF} = 0$ between the $\Delta = 0$ and the paired phase, the quantity $\chi(0)$ is a function of μ and h only. Here we have $U^{-1} + \chi(0) < 0$, independent of $1/k_F a$. It is easy to show that the expression inside the square brackets of the second line in Eq. (12a) vanishes when $E_{\mathbf{k}} < h$. Therefore, when $\Delta = 0$ but $1 + U\chi(0) \neq 0$, we always have

$$\frac{\partial^2\Omega}{\partial\Delta^2} = -2\left[\frac{1}{U} + \chi(0)\right] > 0. \quad (13)$$

We will argue later that the positivity of $\frac{\partial^2\Omega}{\partial\Delta^2}$ is associated with stability against phase separation. From this and the above inequality, we can conclude that the homogeneous polarized Fermi gas phase in Fig. 1 is stable with respect to phase separation.

B. Second order total derivative $\frac{\mathrm{d}^2F}{\mathrm{d}\Delta^2} > 0$ – Stability of pairing versus normal Fermi gas for fixed N and δN

Next we investigate the total derivative $\frac{\mathrm{d}^2F}{\mathrm{d}\Delta^2}$, for a fixed particle number system. This is equivalent to confining the equations in the hyperplane defined by the two number equations in the parameter space spanned by Δ, μ and h. The

constraints imposed by the number equations (3) exclude the possibility of phase separation or any spatial variation of the order parameter. We will show that $\mathrm{d}^2F/\mathrm{d}\Delta^2 > 0$ provides a stability condition for superfluidity *vis a vis* a polarized normal Fermi gas phase. This is equivalent to the statement that the free energy reaches a minimum when a nontrivial solution ($\Delta \neq 0$) of our equation set is found.

From the number equations, we have

$$0 = \frac{\mathrm{d}N}{\mathrm{d}\Delta} = \frac{\partial N}{\partial \Delta} + \frac{\partial N}{\partial \mu}\frac{\mathrm{d}\mu}{\mathrm{d}\Delta} + \frac{\partial N}{\partial h}\frac{\mathrm{d}h}{\mathrm{d}\Delta}, \tag{14}$$

$$0 = \frac{\mathrm{d}\delta N}{\mathrm{d}\Delta} = \frac{\partial \delta N}{\partial \Delta} + \frac{\partial \delta N}{\partial \mu}\frac{\mathrm{d}\mu}{\mathrm{d}\Delta} + \frac{\mathrm{d}\delta N}{\mathrm{d}h}\frac{\mathrm{d}h}{\mathrm{d}\Delta}, \tag{15}$$

so that

$$\begin{pmatrix} \frac{\mathrm{d}\mu}{\mathrm{d}\Delta} \\ \frac{\mathrm{d}h}{\mathrm{d}\Delta} \end{pmatrix} = \frac{-1}{\frac{\partial(N,\delta N)}{\partial(\mu,h)}} \begin{pmatrix} \frac{\partial(N,\delta N)}{\partial(\Delta,h)} \\ \frac{\partial(N,\delta N)}{\partial(\mu,\Delta)} \end{pmatrix}. \tag{16}$$

Using the chain rule,

$$\frac{\mathrm{d}\Omega}{\mathrm{d}\Delta} = \frac{\partial \Omega}{\partial \Delta} + \frac{\partial \Omega}{\partial \mu}\frac{\mathrm{d}\mu}{\mathrm{d}\Delta} + \frac{\partial \Omega}{\partial h}\frac{\mathrm{d}h}{\mathrm{d}\Delta}, \tag{17}$$

finally, we obtain

$$\begin{aligned} \frac{\mathrm{d}^2F}{\mathrm{d}\Delta^2} &= \frac{\mathrm{d}^2\Omega}{\mathrm{d}\Delta^2} + N\frac{\mathrm{d}^2\mu}{\mathrm{d}\Delta^2} + \delta N\frac{\mathrm{d}^2h}{\mathrm{d}\Delta^2} \\ &= \frac{\partial^2\Omega}{\partial\Delta^2} + \frac{\partial^2\Omega}{\partial\Delta\partial\mu}\frac{\mathrm{d}\mu}{\mathrm{d}\Delta} + \frac{\partial^2\Omega}{\partial\Delta\partial h}\frac{\mathrm{d}h}{\mathrm{d}\Delta}, \end{aligned} \tag{18}$$

where we have used Eq. (17) to simplify this expression.

We plot the total derivative $\mathrm{d}^2F/\mathrm{d}\Delta^2$ at $T = 0$ as a function of polarization in Fig. 2. This figure demonstrates that for all regions on the right side of the $T_c^{MF} = 0$ line in Fig. 1, (where the solution of the gap equation with fixed particle number exists), $\mathrm{d}^2F/\mathrm{d}\Delta^2$ is always positive. It vanishes precisely at this boundary, that is, on the line $T_c^{MF} = 0$, which separates the paired phase and the polarized normal Fermi gas phase. For definiteness, at unitarity, $\mathrm{d}^2F/\mathrm{d}\Delta^2$ vanishes at $p = 0.72$. Above this polarization the system is stable as a normal, unpaired Fermi gas. Extrapolation of $\mathrm{d}^2F/\mathrm{d}\Delta^2$ to the normal Fermi gas side of this line would lead to a negative value, indicating that the paired state is not stable there.

In summary, when a solution of the self-consistent equations (2)-(4) can be found, a paired phase is expected to be more stable than the unpaired Fermi gas phase, both at zero and finite T. This result agrees with what we obtained in the previous subsection III A, but addresses this issue from a different perspective. Here we consider the stability of the paired phase whereas in Section III A we addressed that of the unpaired Fermi gas. We can turn this around to conclude that *the positivity of* $\mathrm{d}^2F/\mathrm{d}\Delta^2$ *does not provide an extra constraint on the stability of the polarized superfluid phase.*

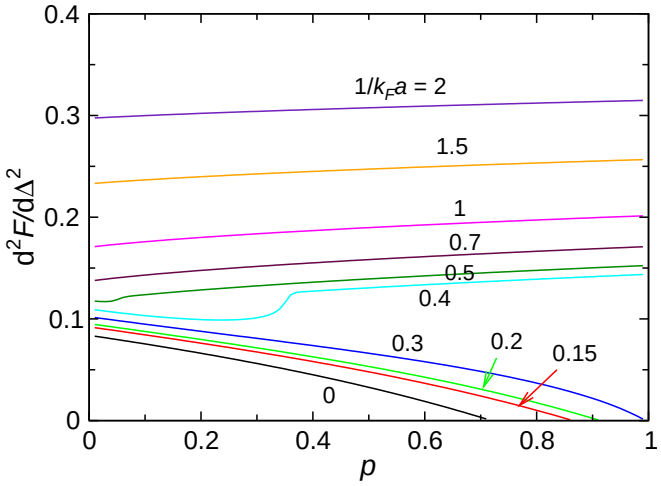

FIG. 2: Behavior of $\mathrm{d}^2F/\mathrm{d}\Delta^2$ at $T = 0$ as a function of polarization p for various interaction strength $1/k_Fa$, from BCS to BEC, as labeled in the figure. From top to bottom, $1/k_Fa$ decreases monotonically. $\mathrm{d}^2F/\mathrm{d}\Delta^2$ remains positive on the right side of the $T_c^{MF} = 0$ boundary in Fig. 1, and vanishes on this boundary.

C. Number susceptibility and stability of homogeneous polarized superfluid against phase separation

In this section, we consider the number susceptibility with respect to variation of the chemical potentials in equilibrium. It is expected on physical grounds [25] that both eigenvalues of the matrix $\partial N_\sigma/\partial\mu_{\sigma'}$ must be positive in order for the system to be stable, against phase separation. It should be obvious that when Δ is held fixed, the eigenvalues of the matrix $\partial N_\sigma/\partial\mu_{\sigma'}$ are always positive. However, when Δ is treated as an implicit function of μ and h as defined by the gap equation (2), the eigenvalues may change sign.

For simplicity in notation, we use partial derivative $\partial/\partial x$ when Δ, μ and h are all treated as independent variables, as in the previous section. When Δ is regarded as a function of μ and h, we define

$$\frac{\mathrm{D}}{\mathrm{D}x} \equiv \frac{\partial}{\partial x} + \frac{\partial\Delta}{\partial x}\frac{\partial}{\partial\Delta}, \qquad (x = \mu, h). \tag{19}$$

With the relationships $N = N_\uparrow + N_\downarrow$, $\delta N = N_\uparrow - N_\downarrow$, and $\frac{\mathrm{D}}{\mathrm{D}\mu_\uparrow} = \frac{1}{2}\left(\frac{\mathrm{D}}{\mathrm{D}\mu} + \frac{\mathrm{D}}{\mathrm{D}h}\right)$, $\frac{\mathrm{D}}{\mathrm{D}\mu_\downarrow} = \frac{1}{2}\left(\frac{\mathrm{D}}{\mathrm{D}\mu} - \frac{\mathrm{D}}{\mathrm{D}h}\right)$, we can easily find

$$\begin{pmatrix} \frac{\mathrm{D}N_\uparrow}{\mathrm{D}\mu_\uparrow} & \frac{\mathrm{D}N_\uparrow}{\mathrm{D}\mu_\downarrow} \\ \frac{\mathrm{D}N_\downarrow}{\mathrm{D}\mu_\uparrow} & \frac{\mathrm{D}N_\downarrow}{\mathrm{D}\mu_\downarrow} \end{pmatrix} = \frac{1}{2}A \begin{pmatrix} \frac{\mathrm{D}N}{\mathrm{D}\mu} & \frac{\mathrm{D}N}{\mathrm{D}h} \\ \frac{\mathrm{D}\delta N}{\mathrm{D}\mu} & \frac{\mathrm{D}\delta N}{\mathrm{D}h} \end{pmatrix} A. \tag{20}$$

Here $A = A^{-1} = \frac{1}{\sqrt{2}}\begin{pmatrix} 1 & 1 \\ 1 & -1 \end{pmatrix}$ is a unitary transformation

matrix. Therefore, the eigenvalues of the matrix

$$M_{2\times 2} = \begin{pmatrix} \frac{\mathrm{D}N}{\mathrm{D}\mu} & \frac{\mathrm{D}N}{\mathrm{D}h} \\ \frac{\mathrm{D}\delta N}{\mathrm{D}\mu} & \frac{\mathrm{D}\delta N}{\mathrm{D}h} \end{pmatrix} \tag{21}$$

are also required to be positive.

From the gap equation, we readily obtain

$$\frac{\partial\Delta}{\partial\mu} = -\frac{\partial\chi/\partial\mu}{\partial\chi/\partial\Delta} = -\frac{\partial^2\Omega}{\partial\Delta\partial\mu}/\frac{\partial^2\Omega}{\partial\Delta^2}, \tag{22}$$

$$\frac{\partial\Delta}{\partial h} = -\frac{\partial\chi/\partial h}{\partial\chi/\partial\Delta} = -\frac{\partial^2\Omega}{\partial\Delta\partial h}/\frac{\partial^2\Omega}{\partial\Delta^2}. \tag{23}$$

It should be noted that this expression is valid only when the gap equation (2) is satisfied, i.e., on the right side of the $T_c^{MF}=0$ boundary in Fig. 1. On the left side, we have the inequality of Eq. (13).

Finally, we have

$$\frac{\mathrm{D}N}{\mathrm{D}\mu} = -\frac{\partial^2\Omega}{\partial\mu^2} + \left(\frac{\partial^2\Omega}{\partial\mu\partial\Delta}\right)^2/\frac{\partial^2\Omega}{\partial\Delta^2}, \tag{24a}$$

$$\frac{\mathrm{D}N}{\mathrm{D}h} = -\frac{\partial^2\Omega}{\partial\mu\partial h} + \frac{\partial^2\Omega}{\partial\mu\partial\Delta}\frac{\partial^2\Omega}{\partial\Delta\partial h}/\frac{\partial^2\Omega}{\partial\Delta^2} = \frac{\mathrm{D}\delta N}{\mathrm{D}\mu} \tag{24b}$$

$$\frac{\mathrm{D}\delta N}{\mathrm{D}h} = -\frac{\partial^2\Omega}{\partial h^2} + \left(\frac{\partial^2\Omega}{\partial\Delta\partial h}\right)^2/\frac{\partial^2\Omega}{\partial\Delta^2}. \tag{24c}$$

Therefore, the eigenvalues are given by

$$\lambda_\pm = \frac{\mathrm{Tr}(M_{2\times 2}) \pm \sqrt{\mathrm{Tr}(M_{2\times 2})^2 - 4\det(M_{2\times 2})}}{2} \tag{25}$$

where $\mathrm{Tr}(M_{2\times 2}) = \frac{\mathrm{D}N}{\mathrm{D}\mu} + \frac{\mathrm{D}\delta N}{\mathrm{D}h}$ and $\det(M_{2\times 2}) = \frac{\mathrm{D}N}{\mathrm{D}\mu}\frac{\mathrm{D}\delta N}{\mathrm{D}h} - \left(\frac{\mathrm{D}N}{\mathrm{D}h}\right)^2$ are the trace and determinant, respectively.

Since $\frac{\partial^2\Omega}{\partial\Delta^2}$ appears in the denominator of the expressions in Eqs. (24), each element of $M_{2\times 2}$ will change sign when $\frac{\partial^2\Omega}{\partial\Delta^2}$ approaches zero and changes sign. Under this circumstance, $[\det(M_{2\times 2})]^{-1}$ approaches zero and changes sign. Our numerics shows that only one of the two eigenvalues in Eq. (25) changes sign. This roughly corresponds to $\frac{\mathrm{D}\delta N}{\mathrm{D}h}$. Therefore, *the stability condition that the eigenvalues of the number susceptibility matrix be positive is equivalent to*

$$\frac{\partial^2\Omega}{\partial\Delta^2} > 0\,, \qquad \text{when} \quad 1 + U\chi(0) = 0\,. \tag{26}$$

This condition has been argued in the literature to correspond to the condition for phase separation. Indeed, this condition says when μ and h are held fixed, a stable homogeneous superfluid solution should always minimize the thermodynamic potential. Otherwise, the system tends to phase separate into a region with smaller Δ and another region with larger Δ, both of which give lower Ω. In such a case, the number density in each region is *not* fixed. Such a phase separation is generally believed to be realized by a one-component Fermi gas physically adjacent to an unpolarized superfluid. We must have $\Delta > h$ in the unpolarized superfluid region. If we take into account the possibility of condensation at $\mathbf{q}_0 \neq 0$, this form of microscopic phase separation may not be the only way to address the instability. One may have a more homogeneous state as well such as found in FFLO-like phases.

The behavior of $\partial^2\Omega/\partial\Delta^2$, the inverse determinant $1/\det(M_{2\times 2}) = 1/(\lambda_+\lambda_-)$ and the eigenvalues of the number susceptibility matrix $M_{2\times 2}$ at $T=0$ are all plotted in Fig. 3 as a function of polarization p for various interaction strengths $1/k_Fa$. From Eqs. (24), it is evident that all elements of the matrix $M_{2\times 2}$ change sign where $\partial^2\Omega/\partial\Delta^2 = 0$. Nevertheless, we notice that one of the two eigenvalues, $EV_1 \equiv \lambda_+$, is always positive. This roughly corresponds to $\mathrm{D}N/\mathrm{D}\mu$. However, the second eigenvalue, $EV_2 \equiv \lambda_-$, does change sign for $1/k_Fa = 1, 1.5$, and 2, exactly where $\partial^2\Omega/\partial\Delta^2 = 0$. Moreover, the fact that $\partial^2\Omega/\partial\Delta^2$ appears in the denominator in Eqs. (24) is manifested by the jump in $\lambda_\pm$ upon the sign change.

If one extrapolates $\partial^2\Omega/\partial\Delta^2$ in the upper left panel, for $1/k_Fa \lesssim 0.3$, one would see that this partial derivative becomes positive above the $T_c^{MF}=0$ line in Fig. 1. This reconfirms that the polarized normal Fermi gas phase in Fig. 1 is stable. One can see thus that the $T_c^{MF}=0$ provides another $\partial^2\Omega/\partial\Delta^2 = 0$ (at $\Delta\to 0$) line, but this time on the BCS side of the resonance. Note the contrasting behavior of $\partial^2\Omega/\partial\Delta^2$ and $\mathrm{d}^2F/\mathrm{d}\Delta^2$ across the $T_c^{MF}=0$ line.

At this stage it is useful to compare with the literature. It is argued in Ref. [26] that the positivity of eigenvalues of the matrix $M_{2\times 2}$ is a necessary but not sufficient condition for stability. Moreover, in this previous work, the positivity of eigenvalues of the number susceptibility matrix was found to be different from the condition contained in Eq. (26). By contrast, here we find that these two conditions are indeed equivalent. The same observation was made in Ref. [21], although only the matrix element $\mathrm{D}\delta N/\mathrm{D}h$ was addressed.

In other recent work [16, 17], a numerical optimization procedure was invoked in which the entire landscape of Ω as a function of Δ for fixed μ and h was used to find the most stable phase. It was argued that $\partial^2\Omega/\partial\Delta^2 = 0$ often gave multiple solutions, sometimes corresponding to a local maximum. In such cases, the $\Delta = 0$ solution was sometimes claimed to be more stable, since it minimizes Ω globally.

These results should be contrasted with the present calculations. Except for the trivial $\Delta = 0$ solution, we find there is at most one solution to our set of equations at either zero or finite T. We argue that the optimization method is in principle valid, but it requires that the system be in chemical equilibrium with an infinitely large particle reservoir so that μ and h are unchanged before and after a possible phase separation. Because the atomic Fermi gases constitute a finite system, μ and h will be different before and after phase separation; they, thus, no longer satisfy the same particle number constraint. In this way we conclude that one cannot use a single $\Omega(\Delta)$ curve to find the solution for the stable phase for a given polarization at fixed particle number.

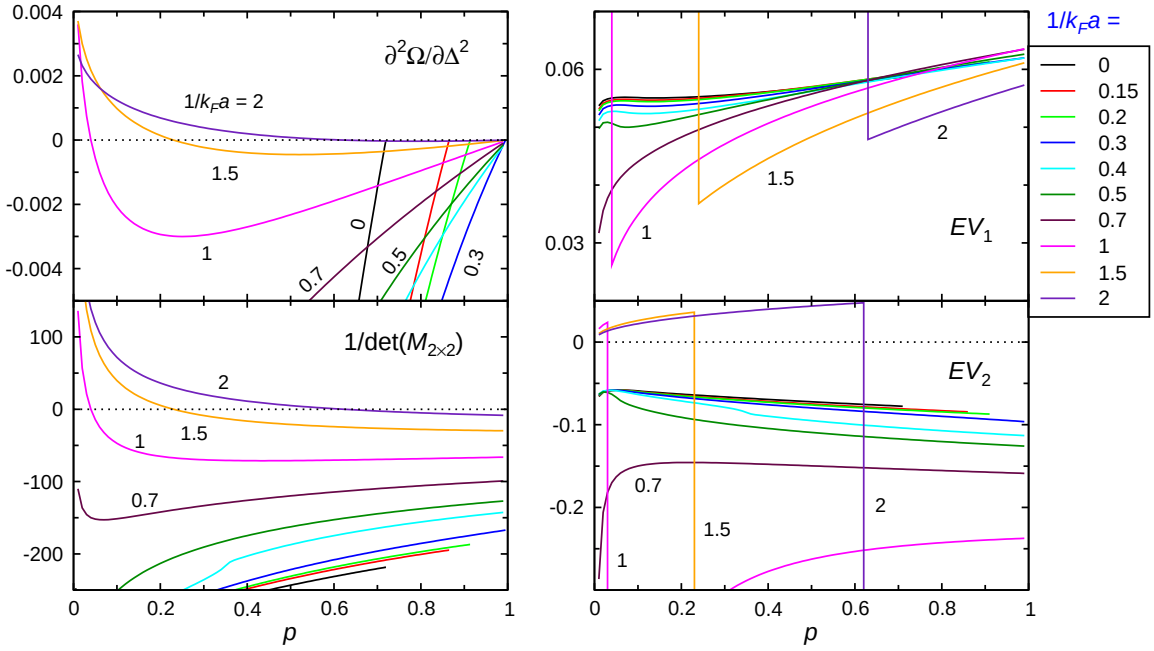

FIG. 3: Behavior of $\partial^2\Omega/\partial\Delta^2$, the inverse determinant $1/\det(M_{2\times2})$ and the eigenvalues of the number susceptibility matrix $M_{2\times2}$ at $T=0$ as a function of polarization p for various interaction strength $1/k_Fa$, from unitarity to BEC, as labeled in the figure. The first eigenvalue, $EV_1 \equiv \lambda_+$, remains positive, roughly corresponding to $\mathrm{D}N/\mathrm{D}\mu$. The sign change of $\partial^2\Omega/\partial\Delta^2$ and the second eigenvalue, $EV_2 \equiv \lambda_-$, and thus $1/\det(M_{2\times2})$ occurs simultaneously, for $1/k_Fa = 1, 1.5$ and 2 on the BEC side of the Feshbach resonance, along the $\partial^2\Omega/\partial\Delta^2 = 0$ phase boundary in Fig. 1.

D. Superfluid density

For a superfluid state to be stable, another obvious condition [25] is that the superfluid density must be positive. Using linear response theory, one can calculate the superfluid density via the response of the system to an external (fictitious) vector potential, as if it were a charged superconductor. In this way one computes the the current-current correlation functions compatible with our T-matrix approximation [28], as shown in Ref. [36]. Here, however, we need to keep track of the population imbalance. Without showing the details, our superfluid density is given by

$$\begin{aligned}\frac{n_s}{m} &= \frac{2}{3}\sum_{\mathbf{k}}\frac{\Delta_{sc}^2}{E_{\mathbf{k}}^2}\left[\frac{1-2\bar{f}(E_{\mathbf{k}})}{2E_{\mathbf{k}}}+\bar{f}'(E_{\mathbf{k}})\right] \\ &\quad\times\left[\varphi_{\mathbf{k}}^2(\nabla\xi_{\mathbf{k}})^2-\frac{1}{4}(\nabla\xi_{\mathbf{k}}^2)\cdot(\nabla\varphi_{\mathbf{k}}^2)\right] \\ &= n_s^{MF}\left(\frac{\Delta_{sc}^2}{\Delta^2}\right)>0\,, \end{aligned} \tag{27}$$

where n_s^{MF} is an artificial construct corresponding to the superfluid density in a BCS-like strictly mean-field treatment. The boundary $n_s = 0$ at $T = 0$ is given by the red line in Fig. 1. This line is completely in the fermionic regime ($\mu > 0$) and within the phase boundary set by $T_c^{MF} = 0$ and $\partial^2\Omega/\partial\Delta^2 = 0$. The superfluid density is positive on the right side of this line, and negative otherwise. We may summarize. The positivity of n_s is a much weaker constraint than that given by Eq. (26), corresponding to the positive definiteness of the number susceptibility matrix. This is different from Ref. [21].

It should be noted that at finite $T > T_c$, n_s vanishes identically. However. n_s^{MF} may remain finite as long as the mean-field equations (2) and (3) are satisfied. In this case, n_s^{MF} may change sign.

Our numerical result shows that the $n_s = 0$ line shifts to the upper left in the $p-1/k_Fa$ phase diagram as T increases from zero, and disappears completely slightly below $T/T_F < 0.2$. Based on Fig. 1, we conclude that n_s remains non-negative for $1/k_Fa > 0.5$.

E. Positivity of the effective pair mass

The effective pair mass can be obtained by Taylor expanding the important pair susceptibility $\chi(Q)$ in the form

$$\chi(Q)-\chi(0) = Z\left(i\Omega_m - \frac{q^2}{2M^*}\right)+\ldots. \tag{28}$$

Most theoretical work in the literature on polarized Fermi gases is based on the ground state [25], or at most on a BCS-like mean-field treatment at finite T [21, 35], which does not include noncondensed pairs. Here, by contrast, we include these noncondensed pairs ($\Delta_{pg}^2 \neq 0$) or pseudogap effects [27] which are reflected in the pair propagator (or T-matrix) and its associated dispersion. As a result, we require that the pair mass be positive. This condition appears as another line

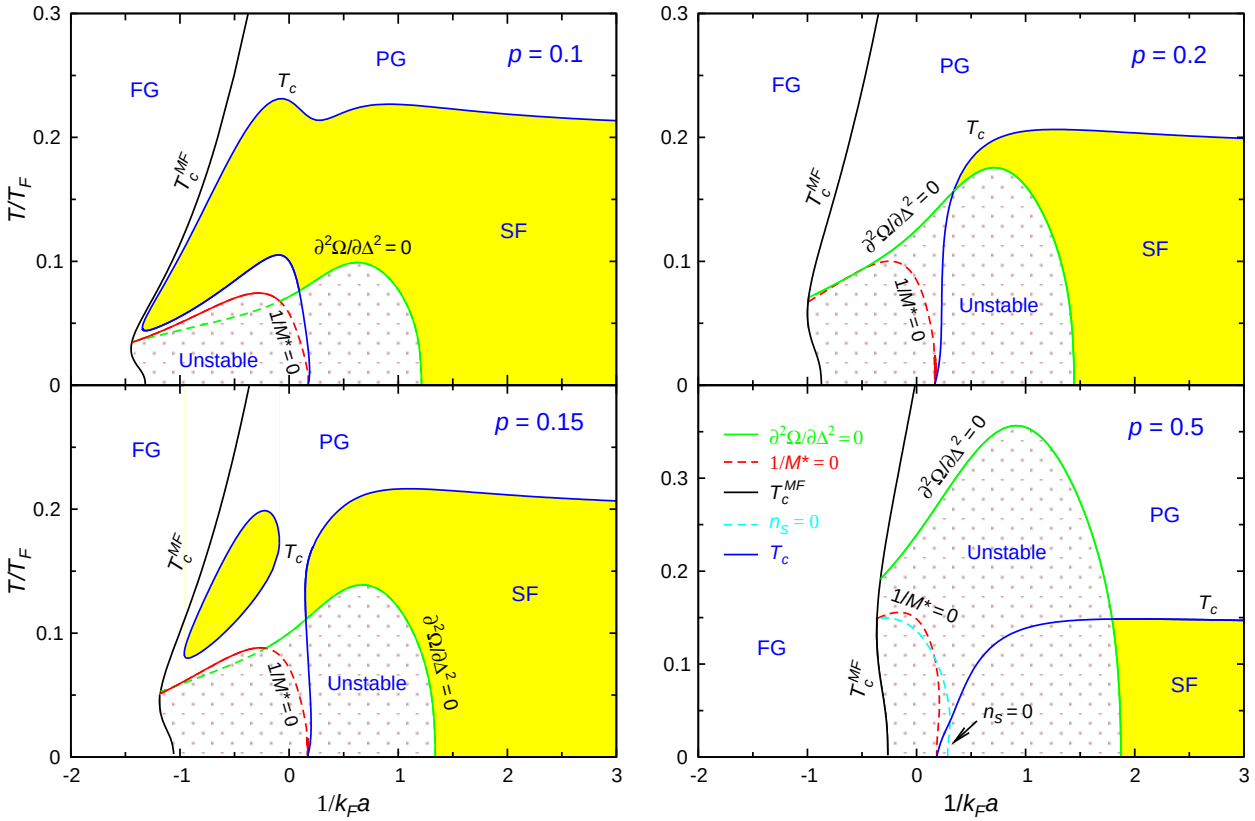

FIG. 4: Phase diagram in the $T - 1/k_F a$ plane for representative values of $p = 0.1$, 0.15, 0.2, and 0.5 (as labeled). Shown are T_c (blue line), T_c^{MF} (black), and the instability boundaries defined by $\partial^2\Omega/\partial\Delta^2 = 0$ (green), and $1/M^* = 0$ (red line), respectively. The yellow shaded area represents stable superfluid (labeled by "SF"), the dotted region is unstable. The white open space on the right of the T_c^{MF} line represents a stable pseudogap phase ("PG"), whereas on its left lies the stable unpaired Fermi gas state ("FG"). At $p \approx 0.14$, the superfluid region splits into two, and the small closed region shrinks with increasing p, and disappears at $p \approx 0.18$. For $p = 0.1$ and 0.15, the two instability lines intersect with each other, whereas for $p = 0.2$ and 0.5, $1/M^* = 0$ is completely inside the unstable region defined by $\partial^2\Omega/\partial\Delta^2 < 0$. The (segment of each) stability line appear as a dashed line when it is inside an unstable region defined by the other stability condition. We also show the line on which $n_s = 0$ (cyan dashed curve) but for $p = 0.5$ only since it is always inside the unstable region.

in the phase diagram of Fig. 1. At $T = 0$, this would correspond to the blue $T_c = 0$ line, which, at this temperature, is completely inside the unstable regime and does not provide an extra constraint. However, at finite T, this line moves considerably to the BCS side, especially at low p. As will be shown below, at low T and low p, this imposes a more stringent constraint than Eq. (26) in the BCS regime.

IV. TEMPERATURE DEPENDENCE OF THE PHASE DIAGRAM

Since superfluidity is essentially a finite temperature phenomenon, it is important to assess the stability of the various superfluid phases at $T \neq 0$. This is where experiments are performed. Our theory allows us to calculate the superfluid transition temperature T_c in the presence of the pseudogap effects associated with incoherent finite center-of-mass momentum pair excitations. We will see that quite systematically, superfluid phases which are unstable at zero temperature, may become stable at finite T. As discussed in Ref. [24] these intermediate temperature superfluids will behave somewhat differently depending on whether they occur to the right or the left of the $T_c = 0$ quantum critical point line in Fig. 1.

In Fig. 4 we present a slice of the finite temperature phase diagram, plotted as characteristic temperature versus $1/k_F a$, at four representative polarizations, $p = 0.1$, 0.15, 0.2 and 0.5. The lines in the figures correspond to T_c and the phase boundaries defined by the instability conditions, including where pairs are no longer found to be stable (via $1/M^* < 0$). The shaded regions indicate where stable superfluidity is found. The dotted regions indicate where either the phase separation stability criterion (given by $\frac{\partial^2\Omega}{\partial\Delta^2} > 0$) is violated, or the effective pair mass becomes negative. It is important to note that on the BCS side of resonance (depending on the polarization) there may be two values of T_c for each value of $1/k_F a$. The meaning of these two T_c's was discussed in earlier work [24]. This case applies to the unitary regime, as should be seen in the figure. Below the lower T_c we find no solution to our set of four equations (2)-(4). In this way the system cannot support superfluidity. More concretely, the effective pair chemical potential become negative below the lower T_c. (At even lower

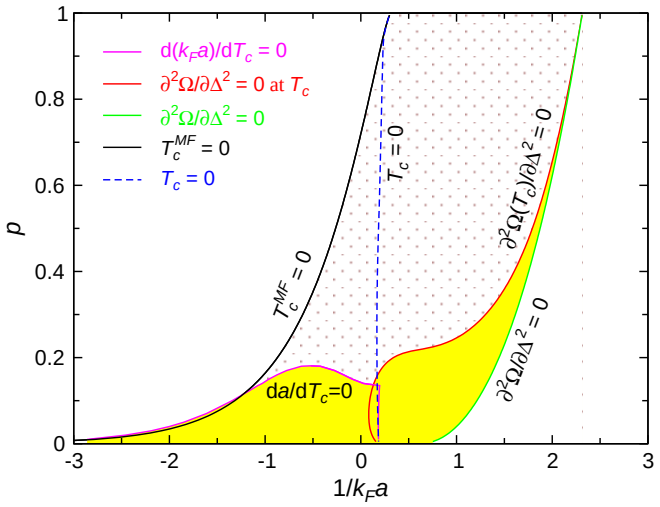

FIG. 5: Phase diagram in the $p - 1/k_F a$ plane, showing where intermediate temperature superfluidity (shaded region) exists. The $T_c^{MF} = 0$, $T_c = 0$, and zero temperature $\partial^2\Omega/\partial\Delta^2 = 0$ lines are the same as in Fig. 1. The red curves represent where $\partial^2\Omega/\partial\Delta^2 = 0$ at corresponding T_c. The line defined by $\mathrm{d}(1/k_F a)/\mathrm{d}T_c = 0$ is given by the turning points $(p, 1/k_F a)$ where $1/k_F a$ reaches a local extremum as a function of T_c. At $T = 0$, the entire region between the $T_c^{MF} = 0$ and the $\partial^2\Omega/\partial\Delta^2 = 0$ lines is unstable against phase separation. However, a stable polarized, intermediate temperature superfluid phase exists for the yellow shaded region enclosed by the (orange) $\mathrm{d}(k_F a)/\mathrm{d}T_c = 0$ curve and the $p = 0$ axis, or by the (red) $\partial^2\Omega(T = T_c)/\partial\Delta^2 = 0$ and (green) $\partial^2\Omega/\partial\Delta^2 = 0$ curves. Superfluidity in the dotted region is unstable at any temperature.

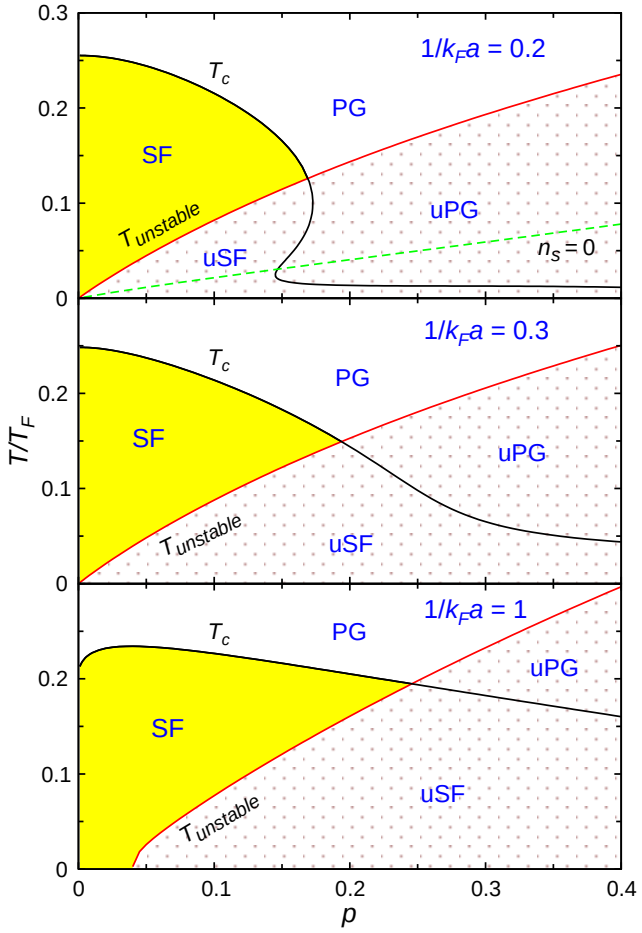

FIG. 6: Behavior of T_c and the instability phase boundary on the BEC side. $T_{unstable}$ is defined by $\partial^2\Omega/\partial\Delta^2 = 0$ in the T-p plane, for $1/k_F a = 0.2$, 0.3, and 1, from top to bottom. For each value of $1/k_F a$, the phase diagram is composed of four different phases, separated by the solid lines: stable superfluid (SF), unstable superfluid (uSF), stable pseudogap (PG), and unstable pseudogap (uPG) phases, as labeled in the figure. The yellow shaded region, on the left of the (black) T_c and (red) $T_{unstable}$ curves, e.g., the shaded area for $1/k_F a = 0.2$, is a stable polarized superfluid. The superfluid solution below these two curves is unstable. Above these two curves, there exists a stable pseudogap phase. The unstable phases will disappear when $1/k_F a > 2.3$. The pair mass is always positive for $1/k_F a > 0.2$. We also show for $1/k_F a = 0.2$ the $n_s = 0$ line, which is completely within the unstable region defined by Eq. (26). n_s does not change sign at any T and p for $1/k_F a > 0.5$.

T, the effective pair mass becomes negative). Above the upper T_c, superfluidity is destroyed in the usual way by finite temperature effects and the system becomes a normal Fermi gas, which is far from ideal. Here there are still strong pairing correlations giving rise to a pseudogap in the fermionic excitation spectrum.

By contrast as we move towards the BEC regime we find only one T_c, but the stability of the superfluid at low T is cut off because of the negativity of $\frac{\partial^2\Omega}{\partial\Delta^2}$. Finally, sufficiently deep into the BEC regime, a stable superfluid persists for all temperatures (below T_c) including $T = 0$.

These results are summarized in the form of a finite temperature phase diagram in Fig. 5. The shaded region indicates where intermediate temperature superfluidity occurs, while the dotted region corresponds to an unstable superfluid, presumably a LOFF-like or heterogeneous phase. Because there is a regime where two $T_c's$ are evident, as seen in Fig. 4, we indicate the upper boundary of the shaded region by a "turning point condition": $\mathrm{d}(1/k_F a)/\mathrm{d}T_c = 0$.

The condition given by Eq. (26) at T_c is represented by the red curve in Fig. 5. Note that T_c self-consistently along this line.

The next two figures correspond to regions on either side of the quantum critical point $T_c = 0$ in Figs. 1 and 5. The region to the right of this line ("Regions IIB and IID" in Ref. [24]) is further discussed in Fig. 6. It corresponds to the BEC side of resonance above $1/k_F a = 0.2$. On the left of this line ("Regions IIA and IIC" in Ref. [24]) which includes the BCS side of resonance as well as the unitary phase we summarize our findings in Fig. 7 below.

In Fig. 6, we show how T_c and $T_{unstable}$ evolve with p and $1/k_F a$ on the BEC side, where $T_{unstable}$ is the temperature where $\frac{\partial^2\Omega}{\partial\Delta^2} = 0$. We do not show the deep BEC case where the superfluid phase is always stable. Here we plot these two families of curves for $1/k_F a = 0.2$, 0.3, and 1.0, from top to bottom. The upper and lower curves in each panel are for T_c and for $T_{unstable}$, respectively. Each phase diagram is composed of four different phases. Inside the shaded area, above

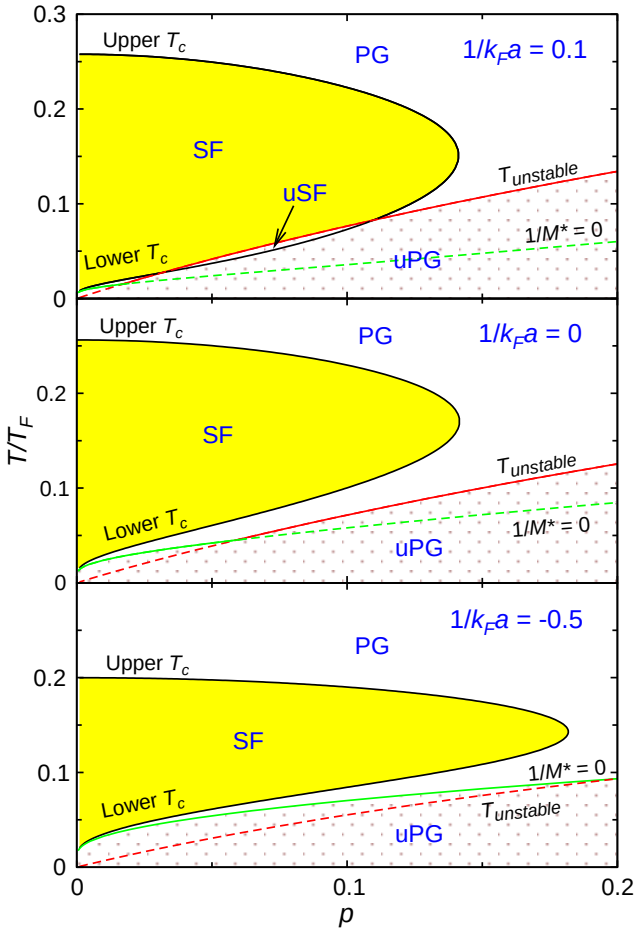

FIG. 7: Phase diagram on the T-p plane on the BCS side of the $T_c = 0$ line in Fig. 1, for $1/k_Fa = 0.1$, 0, and -0.5, from top to bottom. In each panel, the superfluid region is shaded in yellow, on the left side of the T_c curve. Except for $1/k_Fa = 0.1$, the (red) $T_{unstable}$ line does not intersect with the T_c curve. There is a small unstable superfluid phase (uSF) for $1/k_Fa = 0.1$, as labeled in the top panel. For $1/k_Fa = -0.5$, the pseudogap (PG) is present only in a narrow temperature range since here the pair formation temperature T^* (approximately given by T_c^{MF}) is not much higher than the upper T_c. At higher T, the phase is a polarized normal Fermi gas. Slightly below the lower T_c, the pair mass becomes negative (below the green $1/M^* = 0$ line), implying that the paired phase in the mean-field treatment is unstable in this region. The $M^* > 0$ requirement is a tighter constraint than Eq. (26) in the BCS regime at low T and low p.

$T_{unstable}$ but below T_c, there is a stable intermediate temperature superfluid. Below these two curves, the superfluid phase is unstable and this is denoted by "uSF". To the right of the T_c curve we have a stable pseudogap phase above the $T_{unstable}$ line, labeled by "PG". Below the $T_{unstable}$ line we have an unstable pseudogap phase labeled "uPG". When there is a PG phase (stable or unstable) the pairing onset temperature T^* (approximately given by T_c^{MF}, not shown) is higher than T_c. As $1/k_Fa$ increases, the intersection point between $T_{unstable}$ and the $T = 0$ axis moves to the right, and the area of the stable superfluid phase grows, until $1/k_Fa \approx 2.3$, where the area of the unstable phase shrinks to zero. The case $1/k_Fa = 0.2$ is unusual; the T_c curve bends to the left at low temperature. We also show the $n_s = 0$ line for $1/k_Fa = 0.2$. It is completely within the unstable regime, and it disappears for $1/k_Fa \gtrsim 0.5$. The pair mass is always positive for $1/k_Fa > 0.2$.

It should be noted that at a given T below the point where $T_c = T_{unstable}$, there is a critical polarization p_c, above which the superfluid becomes unstable against phase separation (or an FFLO-like pairing state). From Fig. 6, it is evident that p_c increases with T. This trend is consistent with recent experimental results reported by the Rice group [37], which report that the critical polarization for phase separation decreases with decreasing T. In the present work, of course, we have not incorporated the effects of the trap potential. These were discussed elsewhere [30].

We now address Fig. 7 which presents similar plots in the T-p plane for fixed values of $1/k_Fa = 0.1, 0$, and -0.5. This corresponds to the left side of the $T_c = 0$ curve in Fig. 1. Generally, the $T_{unstable}$ curve lies below the corresponding lower T_c curve. The shaded region on the left of the T_c curve in each of the three panels is a stable superfluid phase. For $1/k_Fa = 0.1$, however, the superfluid phase has a tiny region of instability enclosed by the T_c and $T_{unstable}$ curves. As in Fig. 6, the normal region is split into a stable and unstable phase, where pseudogap effects persist except at high T. In all cases, the paired phase below $T_{unstable}$ is unstable. The effective pair mass becomes negative below the line defined by $1/M^* = 0$, which intersects the $T_{unstable}$ line. Here the positivity of the pair mass provides a more stringent constraint on stability than Eq. (26). Finally, just as in Fig. 6, one can find a critical polarization p_c for these values of $1/k_Fa$ as well, and p_c increases with T.

It should be noted that Figs. 6 and 7 evolve smoothly into each other. As $1/k_Fa$ changes continuously from 0.2 to 0.1, the T_c curve at low T in the top panel in Figs. 6 will bend further to the left, and eventually touch the $p = 0$ axis and change into the top panel of Fig. 7.

We end with Fig. 8. This shows how the various phase boundaries first presented in Fig. 1 evolve with temperature. The three panels, from top to bottom, correspond to three different temperatures $T/T_F = 0.05$, 0.1, and 0.2, respectively. The *solid lines* split the phase diagram into a few distinct phases. The points at which T_c^{MF} is equal to the given temperature of each figure lead to a line which separates the unpaired Fermi gas (FG) phase from the paired phases. Similarly, the $T_c = T$ line separates the superfluid phase (below the line) from the pseudogap or normal phases (above the line). Finally, the lines associated with $\partial^2\Omega/\partial\Delta^2 = 0$ and $1/M^* = 0$ separate the stable superfluid and pseudogap phases (below this line) from unstable phases. These two lines intersect with each other, and when this happens, one will appear partly inside the unstable region defined by the other, as indicated by the red and green dashed lines. Thus the stable superfluid phase lies in the yellow shaded region. The $n_s^{MF} = 0$ line (not shown) always appears completely within the unstable phases, and therefore, does not provide a separate phase boundary, as in the $T = 0$ case. (Note here we use n_s^{MF}

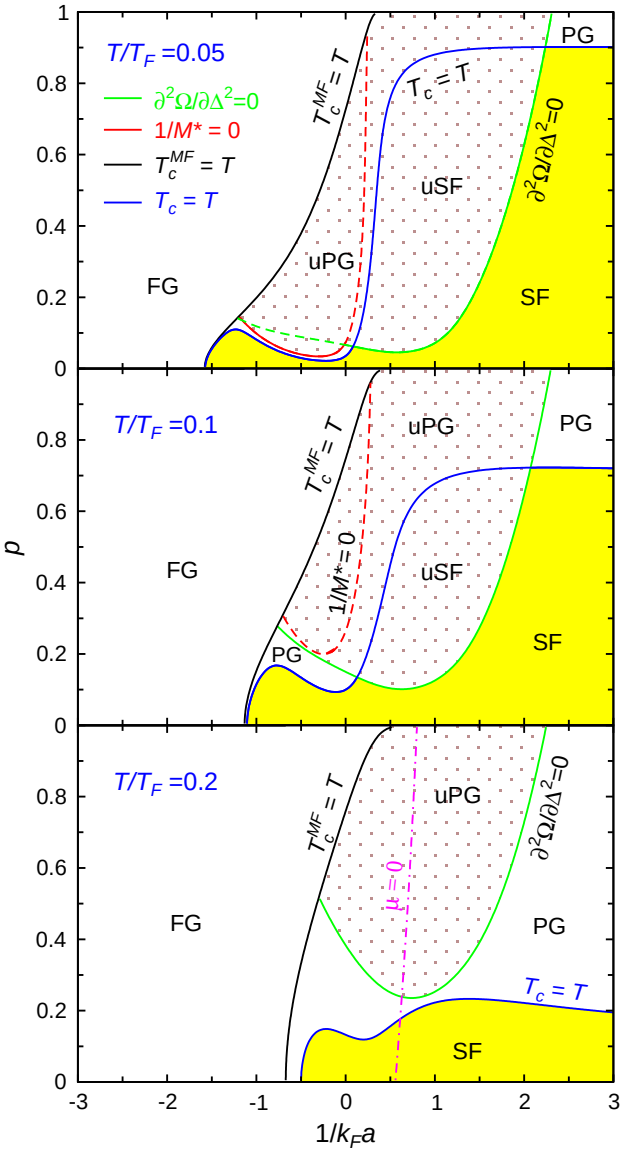

FIG. 8: Evolution of the phase diagram in the $p - 1/k_F a$ plane with temperature. From top to bottom, $T/T_F = 0.05$, 0.1, and 0.2, respectively. The phase diagrams are split into different phases by the solid curves, as labeled in the figure. Except the $\mu = 0$ line (shown for $T/T_F = 0.2$ only) stay relatively unchanged, all other phase boundaries moves with T. The mean-field "phase transition" line, defined by $T_c^{MF} = T$, moves to the right. The (blue) $T_c = T$ line separates the superfluid and the pseudogap (or normal) phase, and the (green) $\partial^2\Omega/\partial\Delta^2 = 0$ line, in conjunction with the (red) $1/M^* = 0$ line, separates the stable and unstable phases. Stable superfluid exists in the yellow shaded region, the dotted region is either an unstable superfluid (labeled by "uSF") or unstable pseudogap ("uPG") phase. The white space on the right of $T_c^{MF} = T$ line is a stable pseudogap ("PG") phase. The $1/M^* > 0$ represents a stronger constraint than Eq. (26) only at low T and low p (e.g., in the top panel). The $1/M^* = 0$ line moves to the upper right and disappears at slightly below $T = 0.2$. The sign change of n_s^{MF} (not shown) always occurs within the unstable regions. We also show $\mu = 0$ which separates fermionic from bosonic regimes.

instead of n_s because $n_s = 0$ outside the superfluid regions.)

As temperature increases, the line associated with $T_c^{MF} = T$ moves to the right. At the same time both the $1/M^* = 0$ curve and the $n_s^{MF} = 0$ curve shrink and move to the upper left, ultimately disappearing slightly below $T/T_F = 0.2$. The $\mu = 0$ boundary between fermionic and bosonic regimes is rather insensitive to T, and so is indicated just for the case of the highest temperature.

The evolution of the $T_c = T$ and $\partial^2\Omega/\partial\Delta^2 = 0$ curves is rather interesting. For low polarization p, both curves move to the left into the BCS regime. This reflects the fact that temperature stabilizes the paired and superfluid phase. This is consistent with our observation of intermediate temperature superfluidity in the presence of population imbalance. The $T_c = T$ curve on the BEC side is continuously suppressed by raising T. This is simply due to fact that T_c decreases with p for given $1/k_F a$ in this regime. In contrast with the $T = 0$ case, we have a stable pseudogap phase appearing at finite T. This corresponds to the white region on the right of the $T_c^{MF} = T$ line, below the $\partial^2\Omega/\partial\Delta^2 = 0$ and $1/M^* = 0$ lines, and above the $T_c = T$ line. At $T/T_F = 0.2$, the $\partial^2\Omega/\partial\Delta^2 = 0$ and the $T_c = T$ lines do not intersect each other, so that the entire superfluid phase is stable.

V. CONCLUSION

In summary, in this paper we have studied the stability conditions for polarized fermionic superfluids in considerable detail. We have restricted our attention to zero momentum condensate pairs, thereby, excluding FFLO-like phases. We find that the positive definiteness of the number susceptibility matrix is equivalent to the positivity of $(\partial^2\Omega/\partial\Delta^2)_{\mu,h}$, provided the gap equation (2) is satisfied. In addition, we find that the positivity requirement of the effective pair mass constitutes another nontrivial stability condition. At low temperature and low population imbalance in the fermionic regime, this latter condition may be more stringent that the positivity requirement of $(\partial^2\Omega/\partial\Delta^2)_{\mu,h}$.

To present our results in a more concrete fashion, we study the phase diagram in different planes of the three-dimensional space spanned by the parameters (T, p, $1/k_F a$). In particular, we have shown how the phase boundaries defined by the various stability conditions evolve with temperature. At relatively low polarization $p \lesssim 0.2$, there exists a stable superfluid phase at finite T, which may not be stable at $T = 0$. In a related fashion, we have shown where on the phase diagram pairing without condensation (that is, a pseudogap phase) appears.

A general observation associated with these population imbalanced theories (which exclude the FFLO phase) is that in the important regime near unitarity, superfluidity only appears at intermediate temperatures [24]. This was seen earlier in mean field approaches [38] via studies of the quantity we define as T_c^{MF}, which was found to be double valued. In the present framework (which goes beyond by including pairing fluctuation effects), this intermediate temperature superfluidity appears via the presence of two $T_c's$ at unitarity. Somewhat above unitarity, and towards the BEC regime, we find

another mechanism for arriving at intermediate temperature superfluidity. This can occur due to a low temperature instability towards phase separation, associated with a negative sign in $(\partial^2\Omega/\partial\Delta^2)_{\mu,h}$.

While $(\partial^2\Omega/\partial\Delta^2)_{\mu,h} < 0$ is argued to lead to phase separation, one may imagine that a negative pair mass would result in a lower pair energy at a finite momentum than at $\mathbf{q}_0 = 0$ and thus a possible LOFF-like condensate. On the other hand, a negative n_s has also been argued [21] to be associated with a LOFF phase. Future studies are needed to unravel these various possible phases within the *unstable* regimes in the phase diagrams.

Acknowledgments

This work was supported by NSF Grant No. PHY-0555325 and NSF-MRSEC Grant No. DMR-0213745

[1] M. Greiner, C. A. Regal, and D. S. Jin, Nature **426**, 537 (2003).
[2] S. Jochim et al., Science **302**, 2101 (2003).
[3] C. A. Regal, M. Greiner, and D. S. Jin, Phys. Rev. Lett. **92**, 040403 (2004).
[4] M. W. Zwierlein, C. A. Stan, C. H. Schunck, S. M. F. Raupach, A. J. Kerman, and W. Ketterle, Phys. Rev. Lett. **92**, 120403 (2004).
[5] M. W. Zwierlein, J. R. Abo-Shaeer, A. Schirotzek, and W. Ketterle, Nature **435**, 170404 (2005).
[6] J. Kinast, S. L. Hemmer, M. E. Gehm, A. Turlapov, and J. E. Thomas, Phys. Rev. Lett. **92**, 150402 (2004).
[7] M. Bartenstein, A. Altmeyer, S. Riedl, S. Jochim, C. Chin, J. H. Denschlag, and R. Grimm, Phys. Rev. Lett. **92**, 203201 (2004).
[8] J. Kinast, A. Turlapov, J. E. Thomas, Q. J. Chen, J. Stajic, and K. Levin, Science **307**, 1296 (2005), published online 27 January 2005; doi:10.1126/science.1109220.
[9] M. W. Zwierlein, A. Schirotzek, C. H. Schunck, and W. Ketterle, Science **311**, 492 (2006).
[10] G. B. Partridge, W. Li, R. I. Kamar, Y. A. Liao, and R. G. Hulet, Science **311**, 503 (2006).
[11] M. W. Zwierlein, C. H. Schunck, A. Schirotzek, and W. Ketterle, Nature (London) **442**, 54 (2006).
[12] E. Gubankova, A. Schmitt, and F. Wilczek, e-print cond-mat/0603603.
[13] W. V. Liu and F. Wilczek, Phys. Rev. Lett. **90**, 047002 (2003).
[14] M. M. Forbes, E. Gubankova, W. V. Liu, and F. Wilczek, Phys. Rev. Lett. **94**, 017001 (2005).
[15] D. Sheehy and L. Radzihovsky, Phys. Rev. Lett. **96**, 060401 (2006).
[16] W. Yi and L. M. Duan, Phys. Rev. A **73**, 031604(R) (2006).
[17] T. N. De Silva and E. J. Mueller, Phys. Rev. A **73**, 051602(R) (2006).
[18] M. Haque and H. T. C. Stoof, cond-mat/0601321 (2006).
[19] J. Kinnunen, L. M. Jensen, and P. Torma, Phy. Rev. Lett. **96**, 110403 (2006).
[20] K. Machida, T. Mizushima, and M. Ichioka, cond-mat/0604339 (2006).
[21] L. Y. He, M. Jin, and P. F. Zhuang, e-print cond-mat/0606322.
[22] C. H. Pao, S. T. Wu, and S. K. Yip, Phys. Rev. B **73**, 132506 (2006).
[23] P. Pieri and G. C. Strinati, Phys. Rev. Lett. **96**, 150404 (2006).
[24] C. C. Chien, Q. J. Chen, Y. He, and K. Levin, e-print cond-mat/0605039; Phys. Rev. Lett. **97**, in production.
[25] C. H. Pao, S. T. Wu, and S. K. Yip, Phys. Rev. B **73**, 132506 (2006).
[26] D. E. Sheehy and L. Radzihovsky, e-print cond-mat/0608172.
[27] Q. J. Chen, I. Kosztin, B. Jankó, and K. Levin, Phys. Rev. Lett. **81**, 4708 (1998).
[28] Q. J. Chen, J. Stajic, S. N. Tan, and K. Levin, Phys. Rep. **412**, 1 (2005).
[29] Q. J. Chen, J. Stajic, and K. Levin, Low Temp. Phys. **32**, 406 (2006) [Fiz. Nizk. Temp. **32**, 538 (2006)].
[30] C. C. Chien, Q. J. Chen, Y. He, and K. Levin, e-print cond-mat/0605684; Phys. Rev. A **74**, in production.
[31] P. Fulde and R. A. Ferrell, Phys. Rev. **135**, A550 (1964); A. I. Larkin and Y. N. Ovchinnikov, Zh. Exp. Teor. Fiz. **47**, 1136 (1964) [Sov. Phys. JETP **20**, 762 (1965)].
[32] R. Casalbuoni and G. Nardulli, Rev. Mod. Phys. **76**, 263 (2004).
[33] A. L. Fetter and J. D. Walecka, *Quantum Theory of Many-Particle Systems* (McGraw-Hill, San Francisco, 1971).
[34] M. Machida and T. Koyama, Phys. Rev. Lett. **94**, 140401 (2005).
[35] K. B. Gubbels, M. W. J. Romans, and H. T. C. S. H. T. C. Stoof, e-print cond-mat/0606330.
[36] I. Kosztin, Q. J. Chen, Y.-J. Kao, and K. Levin, Phys. Rev. B **61**, 11662 (2000).
[37] R. G. Hulet, private communications.
[38] A. Sedrakian and U. Lombardo, Phys. Rev. Lett. **84**, 602 (2000).